Silver electrodeposits in ion-exchanged oxide glasses

S. Roy and D. Chakravorty
Indian Association for the Cultivation of Science, Jadavpur, Calcutta 700 032, India
(Received 17 March 1992; revised manuscript received 31 August 1992)

Silver electrodeposits have been grown within a wide range of oxide glass sytems. The latter are first of all subjected to an alkali-metal–silver-ion exchange reaction. The experimental configuration ensures two-dimensional growth. The fractal dimension of the electrodeposits has been estimated for each sample. Glasses having lithium ions (in the original composition) show a fractal dimension around 1.85 whereas those containing sodium ions give a fractal dimension of 1.68 for their respective silver deposits. Dendritic growth has been observed in glasses containing nanometer-sized metal particles of either bismuth or aluminum. The fractal dimension of all the electrodeposits appears to increase as the length scale is reduced.

I. INTRODUCTION

Growth of electrodeposited metals has attracted considerable attention in recent years because of their fractal geometry and dendritic growth.[1–5] Such growth has been studied extensively as a model for understanding diffusion-limited growth phenomena.[6] Most of the studies involved experiments in which the electrodeposition of the metallic species was carried out by using an aqueous electrolyte with a ringlike anode and a sharp tip cathode forming the electrolytic cell. In order to obviate the problem of convective solvent motion an interesting technique was recently reported in which copper electrodeposits from an acid solution were grown in a solution-damp standard laboratory filter paper.[7,8] The use of a support medium facilitates various characterization measurements besides making it possible to carry out useful experiments in electrocatalysis. We have recently used a silver enriched oxide glass—produced by an ion-exchange reaction—as the medium for growing silver metal by the electrodeposition process. Our objective has been to prepare glass-metal nanocomposites by this novel method.[9] We have now studied in detail the structure, fractal dimension of the metal deposits, etc. in different glass systems. In this paper we report on the experimental technique used and the structural data obtained in various glass-metal systems.

II. EXPERIMENTAL DETAILS

Table I summarizes the glass compositions used as the media for electrodeposition. It should be noted that the glass series indicated by E and F consist of oxide glasses containing dispersoids of metal particles of nanometer dimensions. The microstructural characteristics of these glasses have been discussed earlier.[10,11] The E series glasses contain bismuth particles of nanometer dimensions, whereas glasses in the F series have aluminum particles of similar dimensions. The glasses are melted in alumina crucibles in an electrically heated furnace at temperatures ranging from 1400 to 1600 K. Reagent grade chemicals have been used as raw materials. Molten glasses are poured onto aluminum moulds. Glass samples of approximate dimension $5\times4\times1.5$ mm^3 are cut from the cast pieces. The glass surfaces are polished to optical finish. The samples are subjected to an alkali-metal$\rightleftharpoons$silver-ion exchange reaction by immersing them in a molten bath of silver nitrate at a temperature of 595 K for periods varying from 1 to 50 h. Such a treatment produces a layer of thickness in the range 5–30 μm enriched in silver ions within the concerned glass sample.[12] The ion-exchanged samples are washed in distilled water to remove any silver nitrate adhering to their surfaces. The electrical resistivity of the ion-exchanged layer of different glasses has been estimated from the frequency-dependent capacitance and resistance data obtained from measurements carried out over the temperature range 300–573 K. The details have been discussed elsewhere.[11]

For fractal growth experiments silver paint electrodes (supplied by Acheson Colloiden B.V. Holland) with a separation of 2.0 mm are applied to one surface of the ion-exchanged sample. The configuration of the specimen system is shown schematically in Fig. 1. The sample temperature is first of all raised to a value such that the resistance between the above electrodes is $\sim10^6$ Ω. A dc voltage in the range 1–50 V is applied across the electrodes for a period ranging from a few minutes to $\frac{1}{2}$ h. All the samples show a switching behavior, viz., they switch from a high resistance state to a low resistance one. Successively higher voltages have been applied to the same sample until switching occurs after a maximum duration of $\frac{1}{2}$ h keeping the applied voltage fixed. The switching is evidently brought about by the formation of metallic percolation paths between the two electrodes. The possible mechanism is discussed in the following section. Figure 2 is a typical voltage-current plot showing the switching in the case of glass no. B2 ion-exchanged for 1 h. The duration of electric field application is identical to the time taken by the sample to undergo this switching. The sample is thereafter quenched to room temperature. The structure of electrodeposited silver is studied by both a Leitz optical microscope and a scanning electron microscope, type Hitachi S-415 A.

TABLE I. Composition of glasses used for fractal growth studies (in mole %).

Glass No.	Na_2O	Li_2O	CaO	Al_2O_3	B_2O_3	Bi_2O_3	Al	SiO_2
A1		10	13	3	10			64
A2		20	13	3	4			60
A3		30	12	3				55
B1	10		13	3	20			54
B2	20		13	3	4			60
C1	20			5	75			
E1	23				15	8		54
E2	30				10	8		52
F1	20				60		20	
F2	30				10		20	40

III. RESULTS AND DISCUSSION

Table II summarizes the activation energy for conduction in different ion-exchanged samples, temperature at which electric field is applied to the specimen, its resistance, and the magnitude and duration of the applied electric field. The activation energy has been estimated by fitting the electrical resistivity data to the Arrhenius equation. From the second column in Table II it appears that there is an apparent increase in the estimated activation energy value as the ion-exchange duration is decreased. For shorter ion-exchange treatment the thickness of the silver-rich layer within the glass sample is reduced. As a result the temperature variation of resistivity of the sample is controlled by the unexchanged glass which has been reported to have a higher activation energy than the ion-exchanged sample.[12] It is to be noted therefore that the true measure of the activation energy of the ion-exchanged portion of glass samples is given by the value obtained in the case of samples ion exchanged for maximum duration. From the data in Table II it is evident also that the switching is achieved at lower electric fields in samples ion exchanged for the longest period. This appears to be correlated with the availability of a larger number of silver ions in these specimens. This is also confirmed by the result that in a particular glass system the switching field is lower for glasses containing higher mole percentage of alkali ions and hence having larger concentration of silver ions after the ion-exchange treatment. In this connection it is to be noted that the electric field strength and duration of its application for bringing about this switching effect are smaller in the case of glasses E and F, respectively, as compared to other glass compositions. This arises due to the existence of nanoparticles of bismuth and aluminum, respectively, in these glasses. The latter situation effectively lowers the thickness of the ion-exchanged sample to be covered by the metal chain formation to bring about the switching to a high conducting state. It is to be noted that the switched state is not necessarily stable. A possible mechanism invoking the breakup of metal chains formed by nanoclusters has been discussed earlier.[9]

The mechanism of formation of the metallic percolation paths can be described by the following model.

Silver ions under the influence of the applied electric field migrate from the anode to the cathode where they get reduced to the atomic state after discharge at the electrode. Stable nuclei of metallic silver particles form first at the cathode. The activation energy (the free energy change) ΔF for the formation of such particles can be written as[13]

$$\Delta F = \frac{16\pi\gamma^3}{3(\Delta G_v)^2} , \tag{1}$$

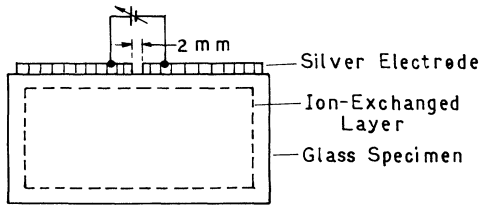

FIG. 1. Sample configuration for electrodeposition experiments.

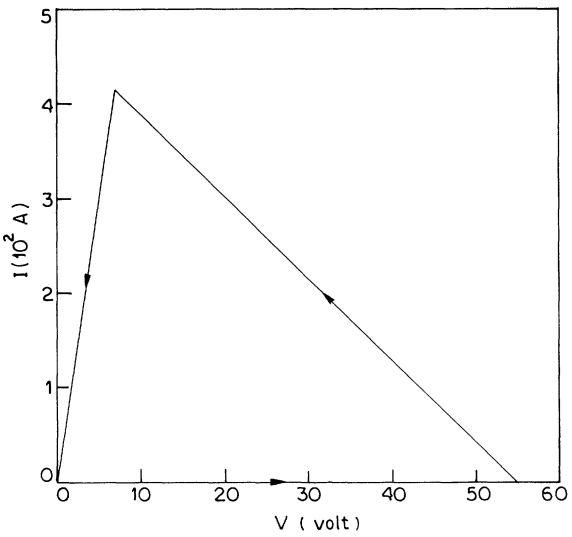

FIG. 2. Typical voltage-current characteristics for ion-exchanged glass no. B2 at 496 K.

TABLE II. Summary of sample characteristics and preparation conditions for electrodeposition of silver in ion-exchanged glasses.

Glass no.	Ion-exchange duration (h)	Activation energy in ion-exchanged sample (eV)	Temperature (K)	Sample resistance (Ω)	Electric field (V/cm)	Duration for applied electric field
A1	50	0.94±0.02	581	15.0×10^6	75.0	6 min
	8	0.99±0.01	572	24.0×10^6	75.0	30 min
	1	1.00±0.01	581	10.9×10^6	275.0	19 min
A2	50	0.66±0.01	568	1.2×10^6	32.0	few seconds
	8	0.85±0.00	535	1.1×10^6	8.5	30 min
	1	0.91±0.01	525	9.9×10^6	275.0	11 min
A3	50	0.50±0.04	461	1.7×10^6	1.0	few seconds
	8	0.64±0.01	478	0.7×10^6	8.5	12 min
	1	0.77±0.01	456	8.1×10^6	175.0	30 sec
B1	8	0.80±0.03	574	13.2×10^6	75.0	15 min
	1	0.88±0.01	587	10.7×10^6	275.0	4 min, 30 sec
B2	50	0.70±0.01	559	0.5×10^6	2.9	few seconds
	8	0.76±0.03	498	9.8×10^6	75.0	3 min
	1	0.79±0.01	496	10.7×10^6	275.0	12 min, 30 sec
C1	8	0.87±0.01	586	16.0×10^6	275.0	30 min (no switching)
E1	8	0.78±0.01	530	12.6×10^6	75.0	2 min
	1	0.85±0.01	560	10.5×10^6	275.0	2 min, 30 sec
E2	8	0.62±0.01	493	5.8×10^6	75.0	5 min
	1	0.70±0.01	487	9.7×10^6	275.0	30 sec
F1	8	0.59±0.01	525	9.2×10^6	75.0	10 sec
F2	8	0.45±0.02	434	10.0×10^6	275.0	10 sec
	1	0.69±0.02	422	11.0×10^6	275.0	3 min, 30 sec

where γ is the energy per unit area of the interface between the metal particle and the glass matrix and ΔG_v is the free energy change per unit volume involving the precipitation of the metallic phase within the glass matrix. According to this model, the radius of the metallic cluster having the maximum free energy is given by

$$r=-\frac{2\gamma}{\Delta G_v}\ . \tag{2}$$

There is thus a possibility of generating a particle size distribution in a narrow range. The percolation of these metallic particles takes place by either a diffusion-limited aggregation (DLA) process or a generalized DLA mechanism. The latter two are discussed further in the next section.

In the light of the model discussed above regarding the formation of metallic percolation paths it is evident that the relationship between the lowering of the switching

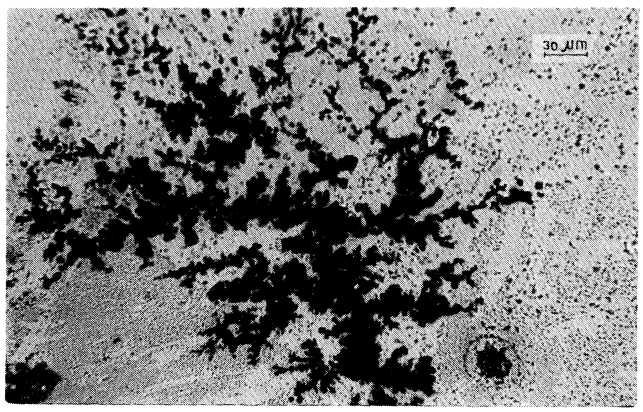

FIG. 3. Optical micrograph of silver deposit in glass A1 ion exchanged for 8 h ×330.

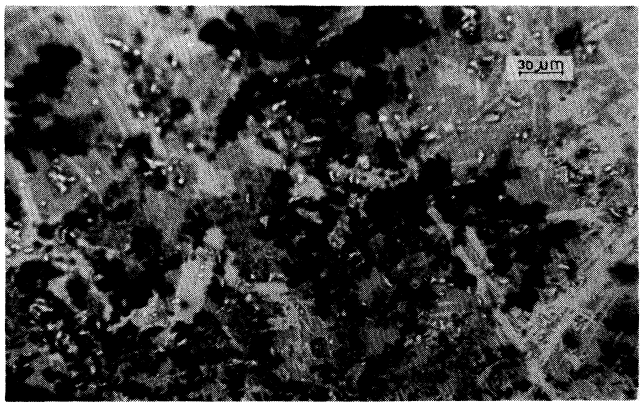

FIG. 4. Optical micrograph of electrodeposited silver in glass A2 ion exchanged for 8 h ×330.

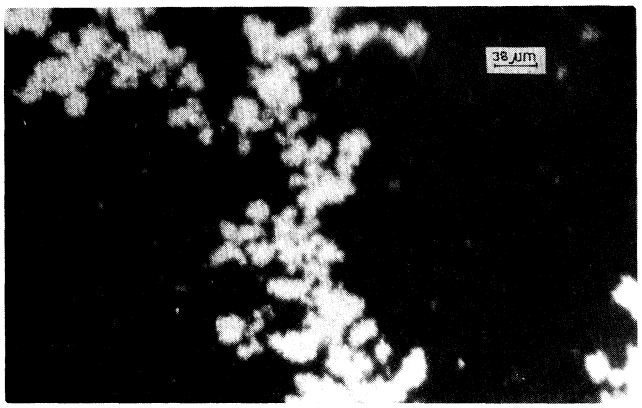

FIG. 5. Optical micrograph of electrodeposited silver in glass A3 ion exchanged for 8 h ×260 (in reflected light).

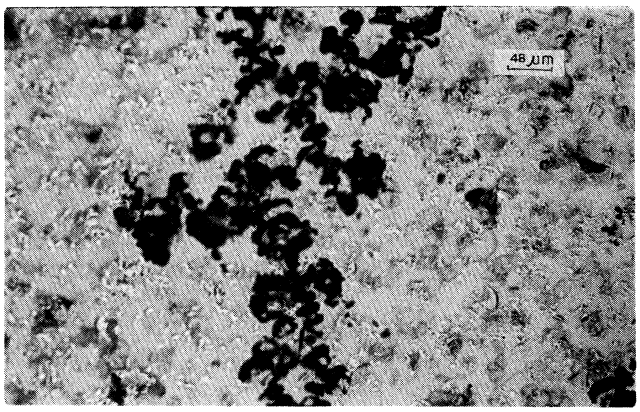

FIG. 7. Optical micrograph of silver deposit in glass B2 ion exchanged for 1 h ×210.

field and its duration and the silver-ion concentration is brought about through the change in the value of the diffusion constant D for the silver ions in the concerned glasses. From the activation energy values listed in Table II it should be obvious that the glasses containing higher concentration of silver ions also have lower activation energies for ionic migration. Using the Nernst-Einstein relation[14]

$$D=\frac{\sigma kT}{Ne^2} \tag{3}$$

$$=\frac{[\sigma_0 \exp(-\phi/kT)]kT}{Ne^2}\ , \tag{4}$$

where D is the diffusion constant, σ the conductivity, k the Boltzmann constant, T the temperature, σ_0 the prefactor in the expression for σ, ϕ the activation energy for ionic migration, N the silver-ion concentration, and e the electronic charge, it is evident that a low value of activation energy ϕ results in an increase in the value of D. This increase is higher than any possible lowering of D value brought about by an increase in the value of N due to compositional changes used in our experiments. A high value of D increases the kinetics of formation of the metallic percolation paths and hence brings about a reduction of both the switching field and its duration.

The explanation delineated as above refers to the switching field and the duration of its application in the case of samples ion exchanged for the maximum period. It should be noted, however, that for any composition the duration of applied field needed for switching becomes longer as the ion-exchange period is reduced. This is believed to arise due to a decrease in the silver-ion flux available at the temperature concerned with a comparable electric field because the effect of the unexchanged glass below the layer of interest becomes substantial even though the overall sample resistance is kept unaltered.

Figures 3–11 show the optical/electron micrographs of silver electrodeposits obtained in different glasses investigated here. We have used optical and electron micrographs interchangeably in our analysis because they give similar results. It is evident that barring glasses in the E and F series all the other glasses exhibit a branched

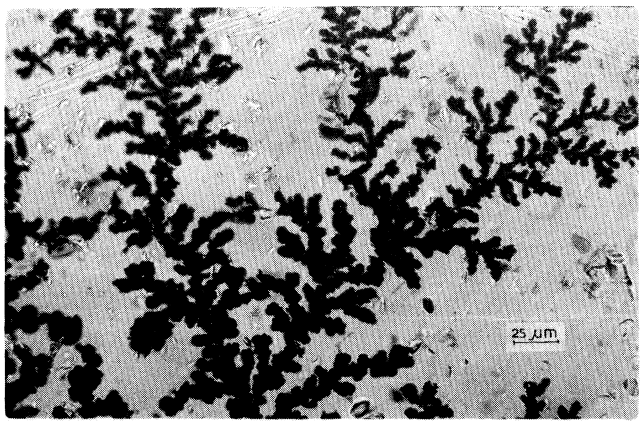

FIG. 6. Optical micrograph of electrodeposited silver in glass B1 ion exchanged for 8 h ×400.

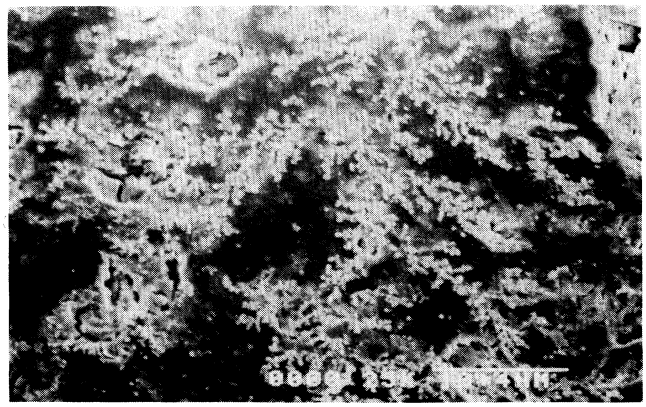

FIG. 8. Electron micrograph of silver deposit in glass C1 ion exchanged for 8 h ×300.

FIG. 9. Optical micrograph of silver deposit in glass E1 ion exchanged for 8 h ×210.

FIG. 11. Electron micrograph of silver deposit in glass F2 ion exchanged for 8 h ×1500.

treelike microstructure. In E and F glasses a dendritic growth pattern is discernible. It should be noted that the ion-exchange duration does not bring about any change in the growth pattern of electrodeposited silver. We have estimated the fractal dimension d_f of the various electrodeposits of silver from the micrographs shown in the above-mentioned figures by the method delineated by Forrest and Witten.[15] The micrograph is first digitized by hand, the presence or absence of particles being indicated by 1's or blanks. The number of particles N in squares of different sizes (l) are counted. The value of the fractal dimension d_f is calculated from the slope of the plot $\log_{10}N$ vs $\log_{10}L$. Figure 12 gives a typical plot of $\log_{10}N$ vs $\log_{10}L$ obtained in the case of fractal structure in glass no. B1 ion exchanged for 8 h. Table III summarizes the d_f values calculated for silver deposits in different glasses. The length scales used in different samples are also indicated in this table.

The higher length scale values indicated for the different samples arise due to the magnification used in taking the concerned micrographs. These values therefore do not indicate the presence of any upper cutoffs to the fractal region. On the other hand, the lower length scale values do represent a lower cutoff below which a loss in self-similarity occurs. Figure 12 shows the lower cutoff point as observed from the experimental data. It is evident from this figure that there is a sharp change in slope of the $\log_{10}N$ vs $\log_{10}L$ curve at a particular value of L which is taken to be the lower cutoff point. The slope in the lower range of L values is calculated to be ~ 1.93. This aspect is further discussed later.

It is evident from the data given in Table III that the values of d_f for silver deposits obtained in a glass after different duration of ion-exchange treatment are identical within the limits of error. Some minor difference is, however, noticeable in glasses B2 and E1, respectively. This could be due to a crossover to higher fractal dimension values as the length scale is lowered. This aspect will be further discussed later.

FIG. 10. Electron micrograph of silver deposit in glass F1 ion exchanged for 8 h ×3000.

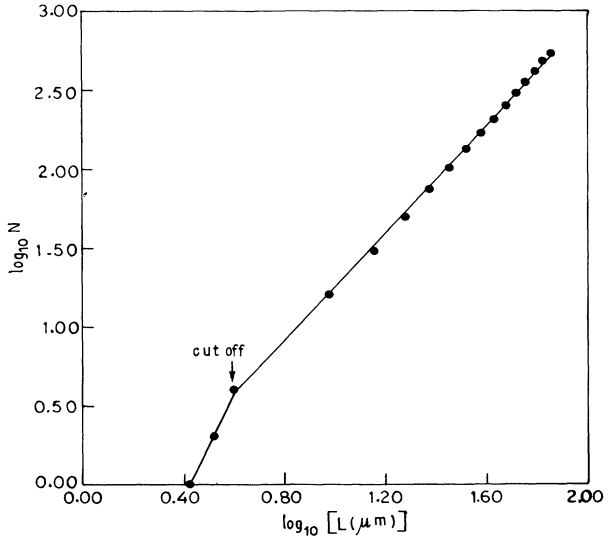

FIG. 12. $\log_{10}N$ vs $\log_{10}L$ for electrodeposited silver in glass no. B1 ion exchanged for 8 h.

TABLE III. Fractal dimensions D of silver electrodeposits as obtained in different glasses.

Glass no.	Ion-exchange duration (h)	Fractal dimension D	Length scale
A1	50	1.83±0.02	24–126 μm
	8	1.86±0.02	24–120 μm
A2	50	1.86±0.01	6–345 μm
	8	1.89±0.02	6–120 μm
A3	8	1.81±0.04	6–114 μm
B1	8	1.77±0.01	4–72 μm
	1	1.72±0.04	2–53 μm
B2	50	1.74±0.02	3–138 μm
	8	1.63±0.02	45–282 μm
	1	1.77±0.02	20–500 μm
C1	8	1.68±0.01	26–200 μm
E1	8	1.79±0.02	90–330 μm
	1	1.85±0.03	16–200 μm
F1	8	1.86±0.03	0.5–10 μm
F2	8	1.52±0.04	1.3–20 μm

From the data summarized in Table III it appears that the fractal dimension of silver deposits in glasses (A1, A2, and A3) containing lithium ions (in the parent composition) has values in the range 1.81–1.89. Glasses B1 and B2, which contain sodium ions in their original composition, on the other hand, give d_f values for their silver deposits around 1.72. The latter is in reasonable agreement with a d_f value of 1.70 as calculated by Witten and Sander on the basis of a diffusion-limited aggregation model. The difference in the d_f values for the two series of glasses is believed to arise due to the ionic size difference of the alkali-metal ions present in these two glass systems, respectively. Because the lithium ion is smaller in size than the sodium ion, the lithium-containing glasses after ion exchange with silver develop higher compressive stress in the exchanged layer than that in the sodium-containing glasses. Glass C1 which has B_2O_3 as the glass network former also gives a d_f value (= 1.67) which conforms to a DLA model.[16]

The higher values of d_f observed in the case of lithium-containing glasses can be explained on the basis of the generalized diffusion-limited aggregation (GDLA) model developed recently by Matsushita *et al.*[17] According to this model the local growth probability $p_g(C_s)$ at a perimeter site C_s of a growing cluster is dependent on the gradient of the random-walker concentration ϕ and is given by

$$p_g(C_s) \sim |\Delta\phi(C_s)|^{\eta} , \tag{5}$$

where η is a positive number determined by the local growth condition. In the present case the growth can be visualized in terms of a simulation schematically shown in Fig. 13. A random walker (a silver ion) is launched from far away. After the arrival of this ion at the site C_s two random walkers (silver atoms) are then launched from C_s which reach the sites C_s' and C_s'', respectively, and occupy those sites, becoming part of the growing cluster. Such a mode of random-walker movement is necessitated by the compressive stress buildup after ion exchange in these glass systems. The mechanism of cluster growth postulated above helps relieve the local stresses without jeopardizing the growth of metal clusters. It has been shown that in a situation like this the value of $\eta=\frac{1}{2}$. The expression for the fractal dimension d_f in the GDLA model is given by[17]

$$d_f = \frac{d_s^2+\eta(d_w-1)}{d_s+\eta(d_w-1)} , \tag{6}$$

where d_s is the dimension of space in which aggregation takes place and d_w the fractal dimension of the random-walker trajectory. Substituting $d_s=d_w=2$ and $\eta=\frac{1}{2}$ in (6) we get $d_f=1.8$. It should be noted that $d_f=1.87$ for $\eta=\frac{1}{3}$, which will correspond to the case of three silver atoms being launched as random walkers for C_s to three other sites on the perimeter of the growing cluster. Release of stress is possible because in the oxide glass structure there are a number of physical voids which can accommodate ions/atoms.[18]

An interesting aspect of the present data is the absence of dendritic growth in the above glass systems though such growth is evident in glasses E1, E2, F1, and F2, re-

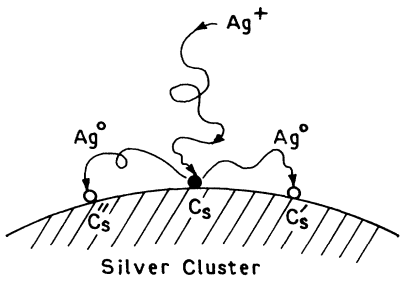

FIG. 13. Schematic representation of GDLA with $\eta=\frac{1}{2}$.

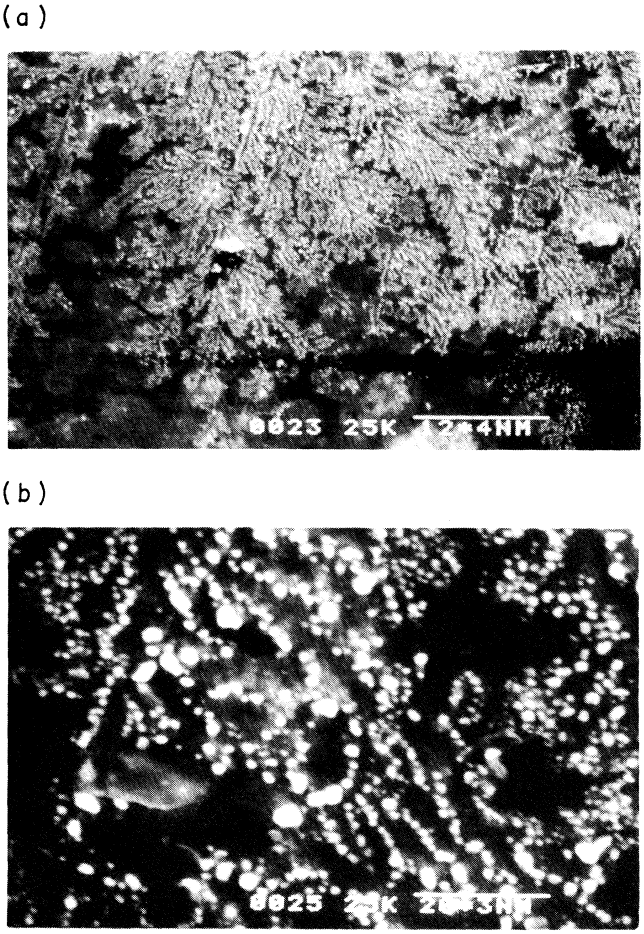

FIG. 14. Electron micrograph of silver deposit in glass B1 ion exchanged for 8 h, (a) ×250; (b) ×1500.

spectively. Dendritic growth has been described as the ultimate limiting form of fractal growth at high voltage.[2,3] In the present investigation high electric field has been used as confirmed by the switching taking place in the ion-exchanged layer as described earlier. Suppression of dendritic growth in glass systems A, B, and C, respectively, implies that the increased mass transport due to fluid motion in a liquid medium[3] is inhibited in a glassy medium. A similar behavior has been reported in the case of electrodeposits produced in a paper medium.[7] Glasses E and F, on the other hand, containing nanometer-sized bismuth and aluminum particles, respectively, give rise to a dendritic growth pattern under high electric field condition. Due to the presence of metal dispersoids in these glasses silver ions participating in the electrodeposition process have to traverse a much smaller distance within the glass structure than that in the previous glass systems before switching occurs. It is believed therefore that in these glass systems increased mass transport over a limited length scale is still possible, thereby giving rise to a dendritic growth pattern.

Another aspect of the electrodeposits studied here is a change in the value of d_f as the length scale is lowered. Figures 14(a) and 14(b) illustrate this point—the figures are scanning electron micrographs for glass no. A1. It is evident that the ramified structure is disjointed in the lower length scale. A value of d_f equal to 1.93 ± 0.04 has been estimated from Fig. 14(b), the length scale being 8–24 μm. This value of fractal dimension is consistent with a d_f value equal to 2 which characterizes the structure of a random image of points.[13] Such a loss of self-similarity is believed to arise due to the breakup of the percolating chains made of metal clusters as a result of localized heating in the switched condition by the passage of electrical current. This also explains why the high conducting state is not stable. It has, however, been possible to retain the percolating chain in certain cases and the electrical behavior of nanometer-sized metal particles constituting such chains studied. These results will be discussed elsewhere.

IV. CONCLUSIONS

Silver electrodeposits can be grown in a wide range of oxide glass systems which have been subjected to an alkali-metal–silver-ion exchange reaction. In glasses containing lithium ions a fractal dimension around 1.85 (length scale 10–300 μm) has been observed whereas in glasses containing sodium ions a value around 1.72 (length scale 3–500 μm) has been found. Borate glasses containing sodium ions give a fractal dimension of 1.68 (length scale 26–200 μm). Though the electrodeposition has been carried out at high electric field, dendritic growth has not been observed in these glass systems. Such growth can, however, be induced in glasses containing nanometer-sized metal dispersoids. All glasses exhibit an increase in the value of fractal dimension at lower length scales.

ACKNOWLEDGMENT

This work has been supported by the Department of Science and Technology, Government of India.

[1]R. M. Brady and R. C. Ball, Nature (London) **309**, 225 (1984).
[2]Y. Sawada, A. Dougherty, and J. P. Gollub, Phys. Rev. Lett. **56**, 1260 (1986).
[3]D. Grier, E. Ben-Jacob, Roy Clarke, and L. M. Sander, Phys. Rev. Lett. **56**, 1264 (1986).
[4]F. Argoul, A. Arnedo, G. Grassean, and H. L. Swinney, Phys. Rev. Lett. **61**, 2558 (1988).
[5]M. Matsushita, M. Sano, Y. Hayakawa, H. Honjo, and Y. Sawada, Phys. Lett. **53**, 286 (1989).
[6]*Fractals in Physics,* edited by L. Pietroniero and E. Tosath (North-Holland, Amsterdam, 1986).
[7]D. B. Hibbert and J. R. Melrose, Phys. Rev. A **38**, 1036 (1988).

[8]D. B. Hibbert and J. R. Melrose, Proc. R. Soc. London, Ser. A **423**, 149 (1989).
[9]S. Roy and D. Chakravorty, Appl. Phys. Lett. **59**, 1415 (1991).
[10]P. Agarwal, S. Roy, and D. Chakravorty, J. Mater. Sci. **26**, 3643 (1991).
[11]D. Chakravorty and T. Mathews, J. Phys. D **22**, 149 (1989).
[12]D. Chakravorty and A. Shrivastava, J. Phys. D **19**, 2185 (1986).
[13]W. D. Kingery, H. K. Bowen, and D. R. Uhlmann, *Introduction to Ceramics* (Wiley, New York, 1976), p. 330.
[14]*Introduction to Ceramics,* Ref. 13, p. 854.
[15]S. R. Forrest and T. A. Witten, Jr., J. Phys. A **12**, L109 (1979).
[16]P. J. Reynolds, H. E. Stanley, and W. Klein, J. Phys. A **11**, L199 (1978).
[17]M. Matshushita, K. Honda, H. Toyoki, Y. Hayakawa, and H. Kondo, J. Phys. Soc. Jpn. **55**, 2618 (1986).
[18]D. Chakravorty and L. E. Cross, J. Am. Ceram. Soc. **47**, 370 (1964).

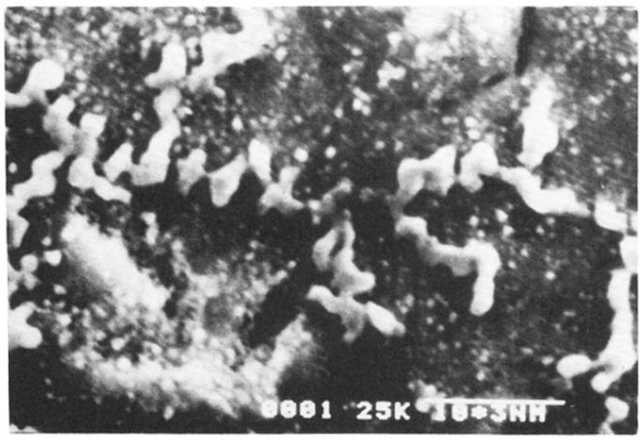

FIG. 10. Electron micrograph of silver deposit in glass F1 ion exchanged for 8 h $\times 3000$.

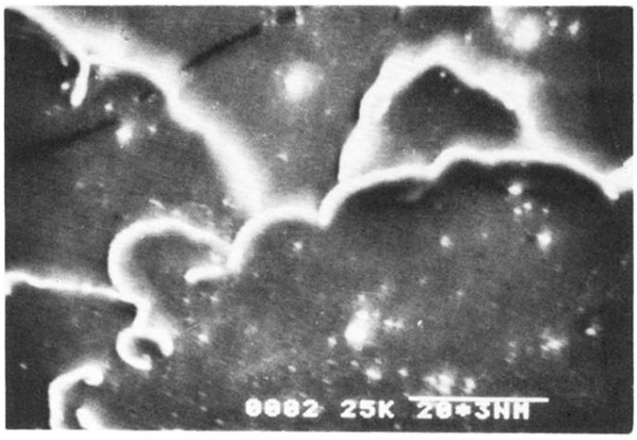

FIG. 11. Electron micrograph of silver deposit in glass F2 ion exchanged for 8 h $\times 1500$.

(a)

(b)

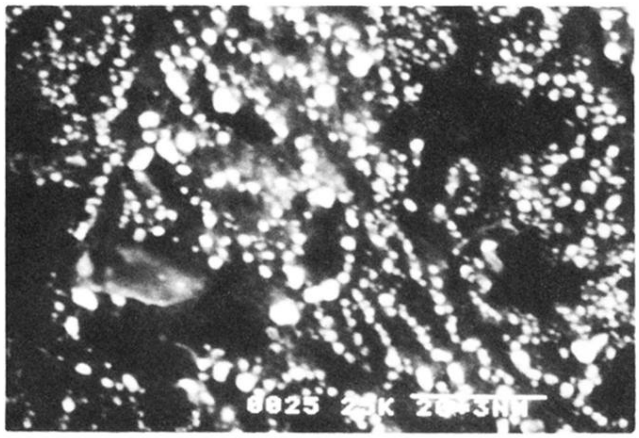

FIG. 14. Electron micrograph of silver deposit in glass B1 ion exchanged for 8 h, (a) ×250; (b) ×1500.

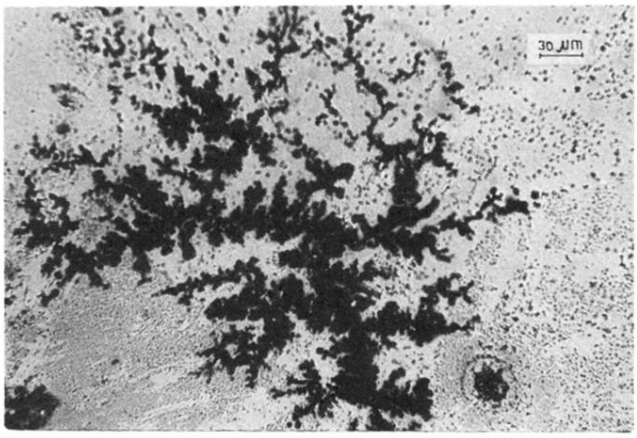

FIG. 3. Optical micrograph of silver deposit in glass A1 ion exchanged for 8 h $\times 330$.

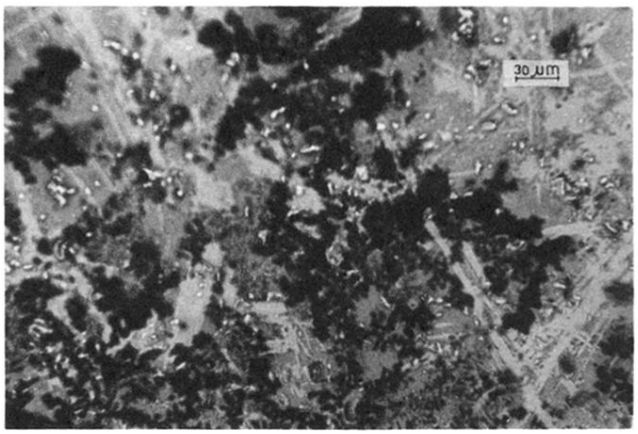

FIG. 4. Optical micrograph of electrodeposited silver in glass A2 ion exchanged for 8 h $\times 330$.

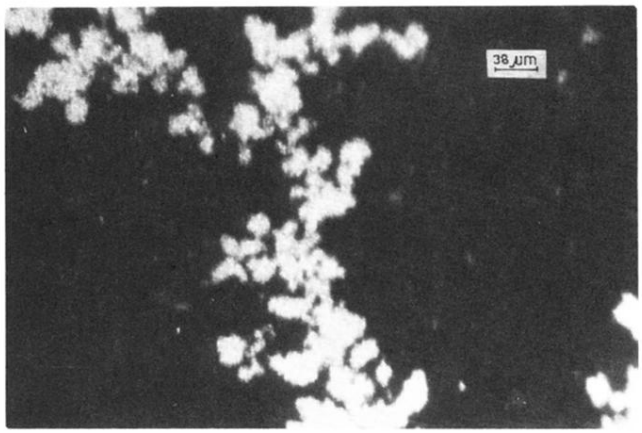

FIG. 5. Optical micrograph of electrodeposited silver in glass A3 ion exchanged for 8 h $\times 260$ (in reflected light).

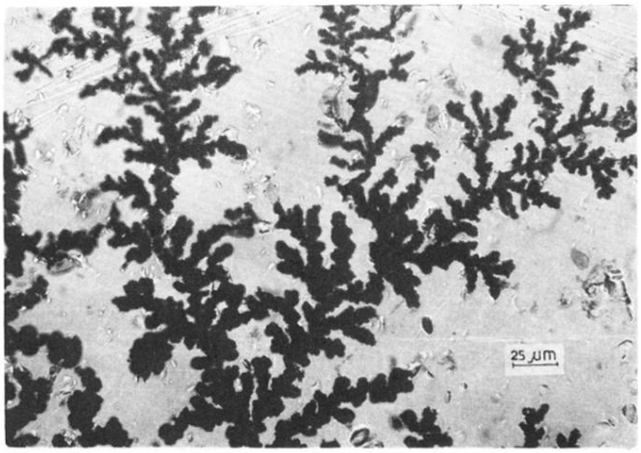

FIG. 6. Optical micrograph of electrodeposited silver in glass B1 ion exchanged for 8 h ×400.

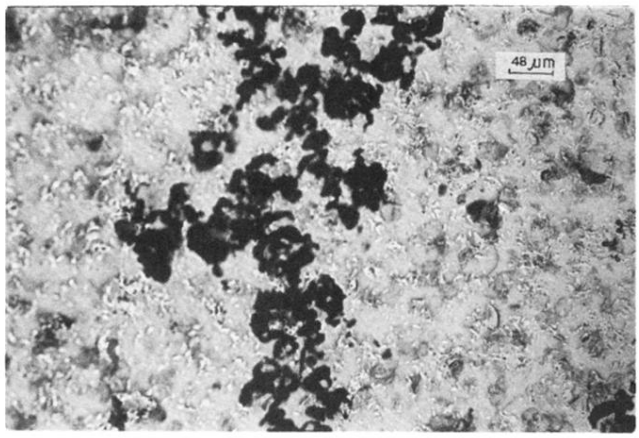

FIG. 7. Optical micrograph of silver deposit in glass B2 ion exchanged for 1 h ×210.

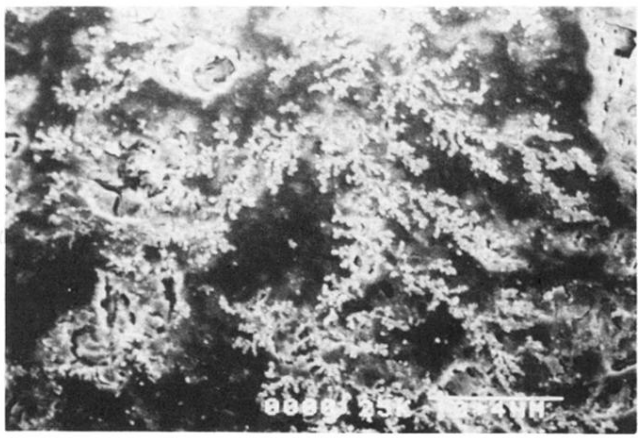

FIG. 8. Electron micrograph of silver deposit in glass C1 ion exchanged for 8 h $\times 300$.

FIG. 9. Optical micrograph of silver deposit in glass E1 ion exchanged for 8 h ×210.